Optical Properties of Aluminum Oxide Compared with Asymptotic Giant Branch Environments from Amorphous to Crystalline Structures

Rakibul A Shohan, Francisco Espinosa-Magaña, Cody Cly, Raul Borja-Urby, Angela Speck, Alan Whittington, Beth Sargent, Joseph Nuth, Arturo Ponce

Microscopy and Microanalysis, **30** (Suppl 1), 2024, 526–528
https://doi.org/10.1093/mam/ozae044.245

Microscopy AND Microanalysis

Meeting-report

Optical Properties of Aluminum Oxide Compared with Asymptotic Giant Branch Environments from Amorphous to Crystalline Structures

Rakibul A. Shohan[1], Francisco Espinosa-Magaña[2], Cody Cly[1], Raul Borja-Urby[3], Angela Speck[1], Alan Whittington[4], Beth Sargent[5,6], Joseph Nuth[7], and Arturo Ponce[1,*]

[1]*Department of Physics and Astronomy, University of Texas at San Antonio, San Antonio, TX, United States*
[2]*Centro de Investigación en Materiales Avanzados S. C., Complejo Industrial Chihuahua, Chihuahua, Mexico*
[3]*Centro de Nanociencias y Micro y Nanotecnologías, Instituto Politécnico Nacional, Mexico City, Mexico*
[4]*Department of Earth & Planetary Sciences, University of Texas at San Antonio, San Antonio, TX, United States*
[5]*Space Telescope Science Institute, 3700 San Martin Drive, Baltimore, MD, USA*
[6]*Center for Astrophysical Sciences, The William H. Miller III Department of Physics and Astronomy, Johns Hopkins University, Baltimore, MD, USA*
[7]*Nasa Goddard Space Flight Center, Greenbelt, MD, United States*

*Corresponding author: arturo.ponce@utsa.edu

Although it is a minor component by mass, cosmic dust plays an outsized role in the universe, contributing to star and planet formation, stellar evolution, and molecule formation to name but a few [1-3]. Optical response is the main mechanism to determine the chemical composition and crystal structure of this cosmic dust. However, many of the dust analogs studied in the laboratory uses materials that are generated in environments very unlike those in space, e.g. [4]. Here we investigate materials created as smoke condensates in systems similar to those expected to generate dust in space to understand their initial structure and how they evolved with annealing. One of the major sources of cosmic dust is Asymptotic Giant Branch (AGB) stars [5]. These stars have been well studied in infrared spectroscopy over the past several decades, but several spectral features remain mysterious or at least controversial. One of the important compounds expected to form around AGB stars in alumina (Al_2O_3). Alumina is a major player in dust condensation mechanisms [6-9]; and is found in presolar grains; meteoritic grains whose isotopic compositions indicate the stellar sources from which they originate [10]. However, since Al is much less abundant than Fe, Si or Mg, alumina's contribution is often overlooked, with the assumption being that its contribution is negligible. Understanding the optical response of Al-O compounds, and how these evolve with annealing is the key to fully understanding dust formation and evolution. The tetrahedron illustrated in figure 1 shows the multiple class of compounds in which oxygen is combined in different forms such as Mg-Al-O, Mg-Al-O-Si, Fe-Al-O, Mg-O-Si, Ca-Al-O, etc. Figure 1B shows the laboratory with sections of precursor used on vapor phase condensates to produce aluminum oxide compound smokes prepared at the Astrochemistry Branch at NASA's Goddard Space Flight Center.

In this work, we have studied aluminum oxide with no other element added to register experimental evidence of optical properties from the amorphous to the most stable crystalline structure alpha-Al_2O_3. The samples were annealed two times, at 900°C for one hour and 1200°C under a rapid thermal annealing. Electron diffraction was performed on the samples before and after annealing shown in figure 2A, 2B and 2C using a JEOL ARM 200F operated at 200kV. The first annealing indicates a crystallization process in which gamma-Al_2O_3 is found, while the second annealing produces the corundum phase, where the number n of clusters $(Al_2O_3)_n$ increases, which leads into the crystalline bulk limit ($n\rightarrow\infty$) [11]. Optical properties of the three samples were measured using electron energy loss spectroscopy (EELS) registered in a JEOL JEM-ARM 200CF microscope operated at 200 kV with cold field emission gun operated in TEM mode with a post-column Gatan imaging filter spectrometer (GIF Quantum 956ER).

The electronic structure of a specimen, which essentially dictates its optical properties, can be determined through the analysis of the outer shell electrons in the low loss region of an EELS spectrum. By applying appropriate deconvolution methods to remove the zero-loss peak, valuable insights into the bandgap region can be obtained while the Kramers–Kronig (K-K) transformation infers the dielectric properties from the measured energy loss function (ELF). The known Al_2O_3 refraction index (1.76) [12] was considered during the application of K–K sum rule to normalize the energy loss function (ELF) and measure thicknesses. There is a relation between the dielectric function (ϵ) and the energy-loss function, $\mathrm{ELF}(E) = \mathrm{Im}\,(-1/\,\varepsilon(E))$, in which ϵ_1 and ϵ_2 can be measured and where Im indicates imaginary part. ELF represents the response of a material to fast electrons traveling through it, as occurs in a TEM–EELS measurement. The dielectric function is a fundamental characteristic that is related in how the material responds to the incident electromagnetic radiation by describing the dielectric constant of a material and the energy dissipation. The energy dependence of the real and imaginary parts of the dielectric function, ϵ_1 and ϵ_2 are shown in figures 3A and 3B. For the complex dielectric function, ϵ_1 is near to unity while the value of ϵ_2 is very small in the high energy edge; ε_1 equivalent to dielectric constant and ϵ_2 corresponds to optical absorption spectra, which provides information of interband transition in the low energy edge, the maxima of ε_2 show predominant transitions. Both real and imaginary parts of the dielectric constant decrease with increasing of photon energy (increasing transmission) as shown in figure 3A and 3B. The ELF spectra can be used to elucidate optical spectra and clearly exhibit the energy range associated with the electronic excitation. Figure 3C shows the ELF spectrum of different configurations of AlO after zero loss peak elimination. The highest peak of the energy loss function is called the plasmon peak of the material. The energies of the plasmon peaks are shift to higher energy during the phase transformation of AlO from amorphous to polycrystalline and crystalline structures. ELF directly reveals the onset of the bandgap energy of AlO samples. In the range of 0 to 10 eV, no definite maxima are observed in the energy loss spectrum due to

the large ϵ_2 in figure 3B. Density-functional theory calculations were performed using the WIEN2k code [13] in order to calculate the frequency dependent dielectric function and compare with EELS measurements. The calculations were performed within the Generalized Gradient Approximation (GGA) exchange-correlation energy in the Perdew-Burke-Ernzerhof (PBE) approach. Calculated real and imaginary parts of dielectric function, as well as energy-loss function are included in figure 3C, where it is evident that the simple annealed at 1200°C give results close to the calculated one at that temperature. Furthermore, the ϵ_1 plots show a zero-crossing with positive slope, indicating a plasmon oscillation at 26.2 eV in the energy-loss function, corresponding to 26.2 eV in calculations. The structural and optical properties measured in the present work are used to be compared with optical properties of aluminum oxide cosmic dust [14].

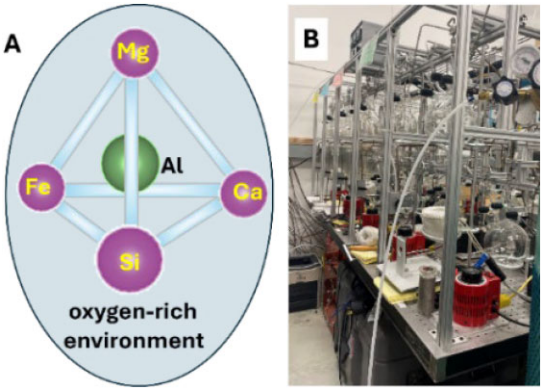

Fig. 1. A) Tetrahedron of aluminum oxygen-rich environments found in asymptotic giant branch (AGB) stars. B) Laboratory of the vapor phase condensate system at the Astrochemistry Branch at NASA's Goddard Space Flight Center.

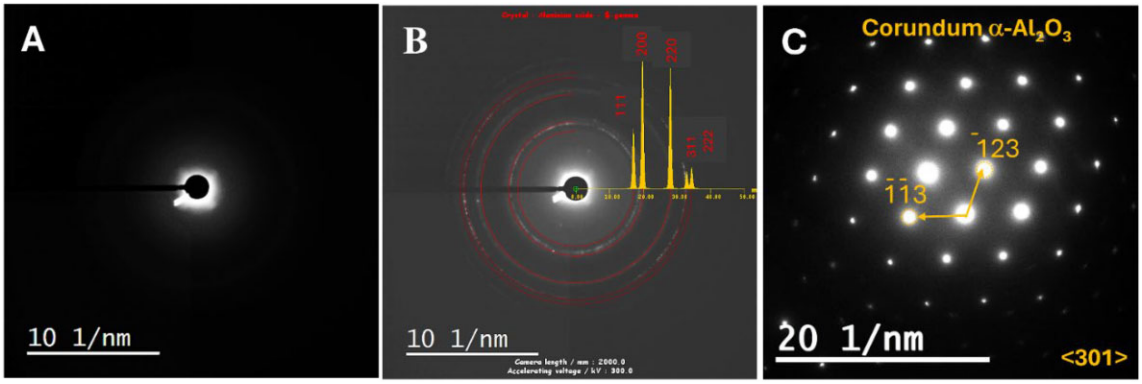

Fig. 2. Structural analysis using electron diffraction of aluminum oxide smokes A) as grown, b) annealed at 900°C for one hour and C) annealed at 1200°C under a rapid thermal annealing.

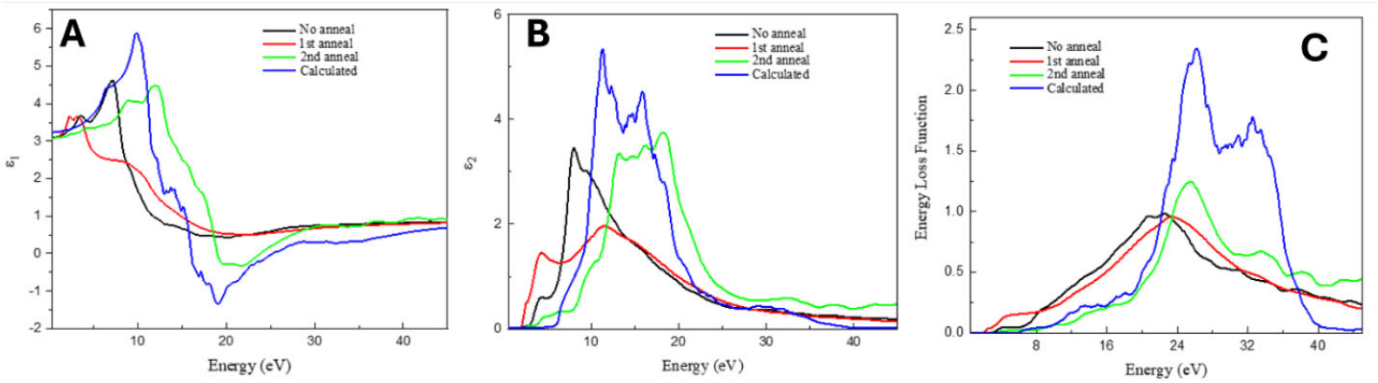

Fig. 3. Optical properties measured from the EELS spectra on the three samples, no annealed, annealed at 900°C for one hour and annealed at 1200°C to a rapid thermal annealing. Calculated properties using alpha-Al_2O_3 are also included in the graphs. Complex dielectric function $\varepsilon(E)= \varepsilon_1(E) + i\varepsilon_2(E)$ including (A) real part ε_1 and (B) imaginary part ε_2, (C) shows the energy loss function (ELF).

References

1. BT Draine, *ARA&A* **41** (2023), **p.** 241. https://arxiv.org/abs/astro-ph/0304489
2. KS Krishna-Swamy **in** "Dust in the Universe: Similarities and differences", (World Scientific Publishing, Singapore).
3. E Krugel **in** "An introduction to the physics of interstellar dust", (Taylor & Francis)
4. J Dorschner *et al.*, *Astronomy and Astrophysics* **300** (1995), **p.** 503.
5. S Kwok, *Nature* **430** (2004), **p.** 985.
6. EE Saltpeter, *Astrophysical Journal* **193** (1974), **p.** 579.
7. K Lodders and B Fegley, *IAUS* **191** (1999), **p.** 279.
8. H-P Gail and E Sedlmayer, *A&A* **347** (1999), **p.** 594.
9. Sargent, ApJL **866** (2018), **p.** 1. https://doi.org/10.3847/2041-8213/aae085
10. DD Clayton and LR Nittler LR, *ARA&A* **42** (2004), **p.** 39.
11. D Gobrecht *et al.*, *A&A* **658** (2022), **p.** 1. https://doi.org/10.1051/0004-6361/202141976
12. J Hwang *et al.*, *Adv. Mater. Interfaces* **1** (2014), p. 1. https://doi.org/10.1002/admi.201400206
13. P Blaha *et al.*, Technische Universität, Wien, Austria, 2001. http://susi.theochem.tuwien.ac.at/

14. The authors acknowledge funding from NSF-AST 2106926 and NASA APRA 80NSSC21K1468